PERMAFROST AND PERIGLACIAL PROCESSES
Permafrost and Periglac. Process., **23**: 292–300 (2012)
Published online 20 November 2012 in Wiley Online Library
(wileyonlinelibrary.com) DOI: 10.1002/ppp.1758

Simulation of the Decadal Permafrost Distribution on the Qinghai-Tibet Plateau (China) over the Past 50 Years

Cheng Weiming,[1]* *Zhao Shangmin,*[2,3,4] *Zhou Chenghu*[1] *and Chen Xi*[2]

[1] State Key Laboratory of Resources and Environmental Information System, Institute of Geographic Sciences and Natural Resources Research, Chinese Academy of Sciences, Beijing, China
[2] Xinjiang Institute of Ecology and Geography, Chinese Academy of Sciences, Urumqi, China
[3] Department of Surveying and Mapping, College of Mining Technology, Taiyuan University of Technology, Taiyuan, China
[4] Graduate University of Chinese Academy of Sciences, Beijing, China

ABSTRACT

Decadal changes in permafrost distribution on the Qinghai-Tibet Plateau (QTP) over the past 50 years (1960–2009) were simulated with a response model that uses data from a digital elevation model, mean annual air temperature (MAAT) and the vertical lapse rate of temperature. Compared with published maps of permafrost distribution, the accuracy of the simulated results is about 85 per cent. The simulation results show: (1) with the continuously rising MAAT over the past 50 years, the simulated areas of permafrost on the QTP have continuously decreased; (2) through areal statistics, the simulated areas of permafrost were $1.60 \times 10^6\,km^2$, $1.49 \times 10^6\,km^2$, $1.45 \times 10^6\,km^2$, $1.36 \times 10^6\,km^2$ and $1.27 \times 10^6\,km^2$, respectively, in the 1960s, 1970s, 1980s, 1990s and 2000s; and (3) the rate of permafrost loss has accelerated since the 1980s, and the total area of degraded permafrost is about $3.3 \times 10^5\,km^2$, which accounts for about one-fifth of the total area of permafrost in the 1960s. Copyright © 2012 John Wiley & Sons, Ltd.

KEY WORDS: permafrost distribution; Qinghai-Tibet Plateau; response model; altitudinal model; mean annual air temperature; vertical lapse rate of temperature

INTRODUCTION

The distribution of permafrost is an important climatic and environmental indicator (Jiang *et al*., 2003), and rising global air temperatures are expected to intensify permafrost degradation (Wu *et al*., 2009). In China, high-altitude permafrost on the Qinghai-Tibet Plateau (QTP) is highly sensitive to climate warming (Li *et al*., 2008), and its degradation is likely to cause many problems relating to engineering, water resource preservation and environmental protection (Jin *et al*., 2000; Cheng & Wu, 2007). Changes in permafrost distribution on the QTP may intensify desertification and affect biochemical processes and human infrastructure. In particular, permafrost degradation may lead to reduced bearing strength of the substrate and increased soil permeability, mass movement and thermokarst activity (Yang *et al*., 2010). Thus, understanding the change in permafrost distribution on the QTP has both scientific and economic significance.

* Correspondence to: C. Weiming, State Key Laboratory of Resources and Environmental Information System, Institute of Geographic Sciences and Natural Resources Research, Chinese Academy of Sciences, Beijing 100101, China. E-mail: chengwm@lreis.ac.cn

Since permafrost distribution cannot be wholly determined from field surveying, computer simulation of its distribution becomes a useful tool (Malevsky-Malevich *et al*., 2001). Therefore, it is important to simulate and dynamically monitor changes in permafrost distribution on the QTP during a long time series. This paper presents data on mean annual air temperature (MAAT) and the vertical lapse rate of air temperature (VLRT). These data, together with a digital elevation model (DEM), are used in the response model of Li and Cheng (1999) in order to simulate and analyse the decadal permafrost distribution on the QTP over the past 50 years.

STUDY AREA

The QTP is located in southwestern China, with the main body in Qinghai Province and the Tibet Autonomous Region. The total area of the QTP is about $2.65 \times 10^6\,km^2$, which accounts for approximately 27.6 per cent of the total area of China (Li, 1987; Zhang *et al*., 2002). As the QTP extends from 73.4°E to 104.5°E and from 25.8°N to 40.0°N, we use Albers projection with two standard parallels of 30ºN and

Received 12 January 2011
Revised 11 October 2012
Accepted 17 October 2012

40ºN and the central meridian is 90ºE, which guarantees minimum deformation (Figure 1).

The QTP is surrounded by several high mountain ranges, including the Kunlun, Altun and Qilian Mountains to the north, the Hengduan Mountains to the east, and the Himalaya and Karakorum to the south and west. There are two relatively flat regions in the middle of the QTP – the Qiangtang Plateau and Qaidam Basin. The former lies in the western QTP and is surrounded by the Kunlun, Bayan Har, Tanggula, Nyainqentanglha and Gandisi Mountains. The latter lies in the northeast QTP and is surrounded by the Kunlun, Altun and Qilian Mountains. A number of large rivers originate on the QTP, including the Yarlung Zangpo, Yellow and Yangtze (Figure 1).

The QTP is much higher than the surrounding areas. Its mean elevation exceeds 4000 m above sea level (asl), and thus it provides an environment for many glaciers and areas of permafrost. Frozen ground on the QTP can be divided into four types: alpine permafrost, predominantly continuous permafrost, isolated permafrost and seasonally frozen ground (Figure 2; Shi, 1988). Alpine permafrost is distributed mainly on the Qilian Mountains and Himalaya, predominantly continuous permafrost on the Qiangtang Plateau, isolated permafrost on the southern and eastern Qiangtang Plateau and seasonally frozen ground mainly in the valleys of the Hengduan Mountains and Qaidam Basin. With climate change, these areas of frozen ground could change type. For example, as the climate warms, the lower limit of permafrost will rise and areas of continuous permafrost may transform to areas of isolated permafrost.

The ground ice content within permafrost on the QTP – an important control on the rate of response of permafrost to climate change – varies in different topographic regions. Low mountains and hilly regions have the highest ground ice content, followed by medium and high mountains; basins and valley plains have the lowest ground ice content (Zhao *et al*., 2010). Overall, the volume of ground ice in permafrost on the QTP is about 9528 km^3.

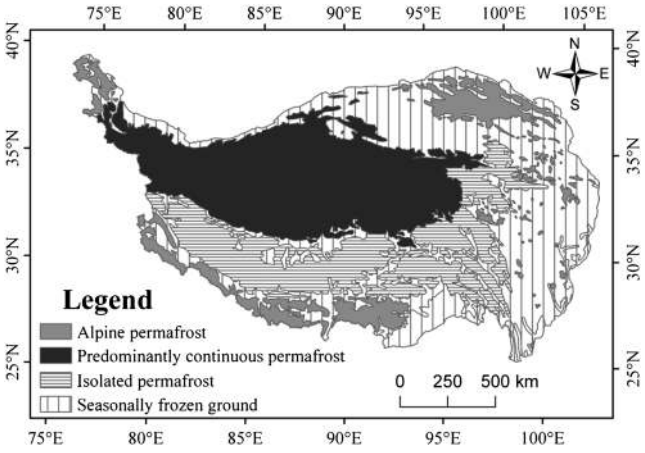

Figure 2 Frozen ground types on the Qinghai-Tibet Plateau (after Shi, 1988).

PERMAFROST SIMULATION MODELLING

Many models have been developed to simulate permafrost distribution. Considering the important role of climate and topographic conditions to permafrost distribution, Markus (1996) presented a computer model to map the probability of permafrost in the Bernese Alps (western Switzerland) based on topographic parameters. Delisle *et al*. (2003) calculated the extent and depth of former permafrost in north-central Europe from MAAT, while Lewkowicz and Ednie (2004) produced a probability map of mountain permafrost using the basal temperature of snow method. Salzmann *et al*. (2007) analysed the validity of using a regional climate model to simulate high-mountain permafrost scenarios, and Bonnaventure *et al*. (2012) presented a regional model to produce a permafrost distribution probability map using a DEM, solar radiation data and other variables. These simulation models mostly focus on larger regions and higher precision, but seldom simulate permafrost distribution over several distinct periods of time, which can show changes in permafrost distribution.

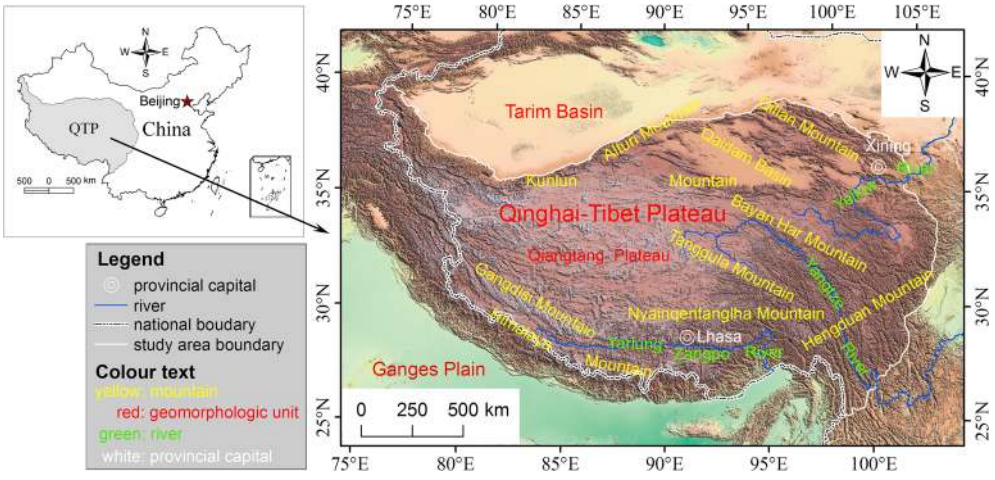

Figure 1 Location and relief shading map of the Qinghai-Tibet Plateau (QTP). This figure is available in colour online at wileyonlinelibrary.com/journal/ppp

Regarding the QTP, Ding and Xu (1982) and Xu and Wang (1983) presented an elevation model to simulate the lower limit of permafrost distribution in both Qinghai and Tibet. Cheng (1984) developed an altitudinal model based on three-dimensional zonation (altitude, latitude and aridity (or longitude)), while Wu *et al.* (2000) compared both of these simulation models on the QTP and concluded that the altitudinal model of Cheng (1984) was more accurate. Based on the altitudinal model (Cheng, 1984), Li *et al.* (1998) built a GIS-based permafrost model to predict permafrost distribution on the QTP in 2009, 2049 and 2099 using air temperature scenario data. Li and Cheng (1999) developed a response model using the GIS-based permafrost model, which provided a way to simulate changes in permafrost distribution on the QTP using air temperature and VLRT data. This response model has been widely used in subsequent research (Jin *et al.*, 2000; Wu *et al.*, 2001; Li *et al.*, 2003; Cheng & Liu, 2008), especially for predicting permafrost distribution, and simulating two or three phases over a long time span. Inevitably, these simulation methods have low precision and much uncertainty. Hence, it is important to simulate permafrost distribution on the QTP in a long time series over the past several decades, evaluating the simulation results against field data or permafrost distribution maps.

In this paper, the simulation method used is the response model presented by Li and Cheng (1999). The permafrost distribution on the QTP has evident characteristics of three-dimensional zonation (altitudinal, latitudinal and aridity (or longitudinal) zones). Through comparison with factors such as the snowline and treeline, the relationship between the lower limit of high-altitude permafrost and latitude can be represented by a curve of the normal frequency distribution formula (Niu, 1980; Jiang, 1982). Using observed data for the lower limit of high-altitude permafrost distribution, the relationship between the altitude of the lower limit and latitude is represented by fitting a Gaussian distribution curve (Cheng, 1984):

$$H = 3650 \ exp \ \left[-0.003 \ (\varphi - 25.37)^2\right] + 1428 \qquad (1)$$

where H is the altitude of the lower limit of high-altitude permafrost and φ *is* the geographical latitude. Equation 1 is referred to as the altitudinal model.

The features of the model are in accordance with the latitudinal distribution of the Earth's radiation budget. Through comparison of the fitted results with measurements, it was found that the accuracy of the model is high (Cheng, 1984). Li and Cheng (1999) compared the simulation results of the altitudinal model and a map of the actual permafrost distribution. Taking 1800 spatial samples for regression analysis, the results showed that the correlation coefficient was 0.92 and the coefficient of determination exceeded 85 per cent. Additionally, the error in the total area was only 1.70 per cent. On the whole, it is feasible to obtain precise simulation results using the altitudinal model.

As the altitudinal model is used to calculate the lower limit of permafrost distribution on the QTP, latitude data are used to compute the elevation of the lower limit of permafrost distribution for each pixel and compare it with Shuttle Radar Topographical Mission (SRTM) data. This relationship can be expressed as the following:

$$P = \begin{cases} 1, & h \geq H \\ 0, & h < H \end{cases} \qquad (2)$$

where P is a Boolean variable, $P = 1$ indicates the presence of permafrost, $P = 0$ indicates the absence of permafrost and h is the altitude of the grid according to SRTM data.

To simulate the dynamic change in permafrost distribution on the QTP, Li and Cheng (1999) proposed a response model based on an altitude model and some assumptions. Referring to the response model, the assumptions in this work are as follows:

(1) Considering the latitudinal stability of the Earth's radiation budget, it is assumed that the Gaussian curves that simulate permafrost distribution do not change because of climate change.
(2) With a change in MAAT, the vertical zonation of permafrost distribution changes by a certain height according to the VLRT, and the lower limit of permafrost distribution changes by the same height, as expressed by Equation 3:

$$\Delta H = \frac{\Delta T}{\gamma} \qquad (3)$$

where ΔH refers to elevation changes, ΔT refers to MAAT changes and γ is the VLRT.

(3) In addition to MAAT and the VLRT, other important factors influence the change in permafrost distribution, such as snow, precipitation and sunshine hours. In this research, however, these factors are neglected for simplification. Additionally, this model is a scenario-type model which cannot consider the lag times during permafrost degradation and formation (Bonnaventure & Lewkowicz, 2010). In fact, although MAAT had changed, permafrost distribution status would be fixed for a longer period.
(4) The total areas of glaciers and lakes on the QTP are about $4.66 \times 10^4\,km^2$ (Li *et al.*, 1986) and $2.42 \times 10^4\,km^2$ (Yang *et al.*, 1983), respectively, whereas the total area of permafrost exceeds $1.20 \times 10^6\,km^2$ (Li & Cheng, 1999). Thus, the areas of glaciers and lakes can be neglected in this simulation. This assumption is reasonable and used in other research (Nan *et al.*, 2005).

DATA ACQUISITION

In this simulation, the main data sources are DEM, latitude and longitude, MAAT and VLRT data.

DEM data are based on SRTM data with a spatial resolution of 3 arc-seconds (SRTM3). Through processing, the spatial

resolution of SRTM3 data is about 500 m, which is the same for other data. According to SRTM3 data, the elevation of the QTP ranges from 83 to 8872 m asl.

Latitude and longitude data are important in determining the three-dimensional zonation of permafrost distribution on the QTP. Furthermore, the latitudinal factor is a variant in the altitudinal simulation model presented by Cheng (1984); both latitude and longitude are closely related to the distribution of MAAT. Through processing, the value of each pixel is the longitude and latitude at the central point of the pixel.

The MAAT is one of the most important climatic factors in the simulation model. MAAT data are obtained from 106 meteorological stations, mainly distributed in the eastern part and northern border of the QTP. Of these stations, 72 are on the QTP, but only 11 in permafrost regions, which may be because the natural environment in the permafrost regions is severe. The sparse distribution of the meteorological stations on the western QTP may affect the precision of the MAAT data. Additionally, air temperature data in surrounding countries, such as Nepal and India, are difficult to obtain and may have consistency problems. Hence, air temperature data for other countries are not used in this work. Statistical values for the elevation and MAAT measurements at the meteorological stations in each decade from the 1960s to the 2000s are presented in Table 1.

Table 1 gives the mean elevation of all meteorological stations as about 3000 m asl. From the 1960s to 2000s, the maximum values of MAAT tend to decrease slightly, whereas the minimum and mean values increase. The values in Table 1 are only statistical values of the measurements made at the meteorological stations, and they cannot present the detailed climatic variation of each region on the QTP. Moreover, some of the meteorological stations are located outside the QTP.

To improve accuracy, linear multiple regression analysis between MAAT, DEM, latitude and longitude data was carried out for each decade. The linear multiple regression equations are presented in Table 2.

As the correlation coefficient (R) exceeds 0.95 and the significance value (Sig.) is 0.000 for each regression equation in Table 2, the MAAT data can be interpolated for the whole QTP using these equations. By computing the difference between the recorded value and simulated value at the meteorological stations, the difference data of MAAT are determined through inverse-distance-weighted interpolation (Bartier & Keller, 1996; Lu & Wong, 2008). The final MAATs are obtained by adding the difference data to the simulation data. The statistical results for MAAT on the QTP in each decade over the past 50 years are presented in Table 3.

Table 3 shows that the climate has continuously warmed since the 1960s, especially in the 2000s, and that the mean value of MAAT on the QTP is now above 0 °C. The continuously warming climate may have resulted in permafrost degradation on the QTP, although the thermal inertia of permafrost and the considerable amount of ground ice within it may have allowed the permafrost to persist for a long time.

The VLRT is an important climatic index representing changes in air temperature with elevation. Using the elevation and air temperature data at equal pressure surfaces of 500, 600 and 700 hPa, a mean annual VLRT isoline map was acquired through kriging interpolation by Li and Xie (2006). The mean elevation on the isoline map is 4500 m asl, which is equivalent to the ground height of the QTP and consistent with the height of the 600 hPa equal pressure surface. Using the VLRT isoline map, VLRT data were acquired through map scanning, geometrical correction, projection, digitisation and interpolation. The final VLRT data range from 0.487 °C/100 m

Table 1 Elevation and decadal values of MAAT at meteorological stations.

		MAAT (°C)				
Statistical value	Elevation (m asl)	1960s	1970s	1980s	1990s	2000s
Maximum	5301.5	19.9	19.8	19.8	19.5	19.3
Minimum	590.5	-5.8	-5.4	-5.5	-5.2	-4.7
Mean	2907.0	5.4	5.5	5.6	6.0	6.4
Standard deviation	1153.9	5.6	5.5	5.5	5.5	5.4

See text for abbreviation.

Table 2 Linear multiple regression equations of MAAT data for each decade.

Decade	Equation	R	Sig.
1960s	MAAT = 573.528 - 0.048 × [SRTM3] - 8.176 × [latitude] - 1.106 × [longitude]	0.959	0.000
1970s	MAAT = 590.464 - 0.047 × [SRTM3] - 8.230 × [latitude] - 1.278 × [longitude]	0.958	0.000
1980s	MAAT = 588.548 - 0.047 × [SRTM3] - 8.148 × [latitude] - 1.281 × [longitude]	0.957	0.000
1990s	MAAT = 582.889 - 0.047 × [SRTM3] - 7.911 × [latitude] - 1.269 × [longitude]	0.956	0.000
2000s	MAAT = 587.115 - 0.047 × [SRTM3] - 7.669 × [latitude] - 1.356 × [longitude]	0.955	0.000

See text for abbreviations.

Table 3 Statistical values of the estimated MAAT (°C) for the QTP in each decade.

Statistical value	1960s	1970s	1980s	1990s	2000s
Maximum	26.0	26.0	26.2	26.4	26.6
Minimum	-19.9	-17.7	-17.7	-17.3	-17.0
Mean	-1.2	-0.7	-0.6	-0.2	0.3
Standard deviation	4.7	4.6	4.6	4.6	4.5

See text for abbreviations.

to 0.699 °C/100 m; the VLRT gradually decreases from north to south. The lower values are distributed in southwestern and eastern areas of the QTP, and the higher values are distributed on the northern QTP, especially around the Altun Mountains.

SIMULATION RESULTS AND ANALYSIS

Simulation Results

As the field survey data for building the altitudinal model were mainly collected in the 1970s, permafrost distribution simulated using this model mainly represents permafrost distribution status in that decade. According to the response model and simulated permafrost distribution in the 1970s, permafrost distribution in other decades of the past 50 years can be simulated using SRTM3, MAAT and VLRT data (Figure 3).

Through areal statistics, the simulated areas of permafrost on the QTP are acquired (Table 4). Figure 3 and Table 4 show that the estimated area of permafrost has continuously decreased over the past 50 years. The area of permafrost that has degraded completely is about $3.3 \times 10^5\,km^2$, which accounts for about one-fifth of the total area of permafrost in the 1960s. The period with the highest rate of permafrost loss is from the 1960s to 1970s, and the area of permafrost loss is $1.1 \times 10^5\,km^2$; the next is from the 1990s to 2000s, and the area is $9.0 \times 10^4\,km^2$.

Change in Permafrost Distribution over the Past 50 Years

Based on the simulation results, changes in the distribution of permafrost and seasonally frozen ground on the QTP were analysed first during each successive two decades and then over the whole 50-year period. The changes are mapped as four categories in Figure 4.

In Figure 4, the category of 'unchanged permafrost' indicates permafrost that has persisted over a particular time period. Such permafrost is mainly distributed in the western and central parts of the QTP and the Qilian Mountains. Second, 'unchanged seasonally frozen ground' (i.e. persistently non-permafrost conditions) is mainly distributed in the eastern and southeastern parts of the QTP and the Qaidam Basin. Third, 'decreased permafrost' (i.e. permafrost that has degraded completely) is mainly distributed at the boundary between the permafrost and non-permafrost regions, the distribution of which was not evident in some periods, such as from the 1970s to 1980s (Figure 4). In this simulation, the change in permafrost distribution is mainly computed from the change in MAAT. Although MAAT values have generally increased during the last 50 years, they may have decreased in some small areas, which may explain some small patches of 'increased permafrost' (i.e. newly formed permafrost).

The changes in area of the four categories above for each decade of the past 50 years are shown in Table 5. Over two successive decades, the area of 'decreased permafrost' is largest from the 1960s to 1970s, followed by the 1990s to 2000s and then the 1980s to 1990s; the area is relatively small from the 1970s to 1980s. The areas of 'increased permafrost' are very small in each period. On the whole, the area of permafrost on the QTP has continuously decreased, and the rate of permafrost loss has accelerated since the 1980s (Table 5).

Over the past 50 years, the area of decreased permafrost far exceeds that of increased permafrost. Hence, the area of permafrost on the QTP has decreased substantially (Table 5). The decreased permafrost is mainly distributed along the southern and eastern borders of the Qiangtang Plateau and in the Yarlung Zangpo Valley and Qilian Mountains (Figure 4e).

DISCUSSION

The actual distribution of the lower limits of permafrost on the QTP is difficult to acquire because we can only determine that the monitoring points are in regions of permafrost or seasonally frozen ground. Previous research about monitoring the permafrost distribution change on the QTP most focus on small parts of the QTP, such as Xidatan (1975–2002; Nan *et al.*, 2003), rather than the whole region. In view of this situation, we compared our simulation results with maps of permafrost and other simulation methodologies.

Comparison between the Simulation Results and Permafrost Maps

The simulation results were firstly compared with the total areas of permafrost shown on published frozen ground maps and then, taking a particular map as an example, the distribution of permafrost shown on it was compared with the simulation results.

The total areas of permafrost shown in various frozen ground maps on the QTP are listed in Table 6. The maps are based on field survey data from different periods and on cartographical generalisation, whereas the simulation model results are based on measurements at meteorological stations.

Comparison of the simulation results with mapped permafrost areas from different time periods indicates that the differences are small. Inconsistencies between the total areas of permafrost shown in Table 6 and the simulation results may be due to several factors, such as differences in map age, boundaries and scale (Wang *et al.*, 2000).

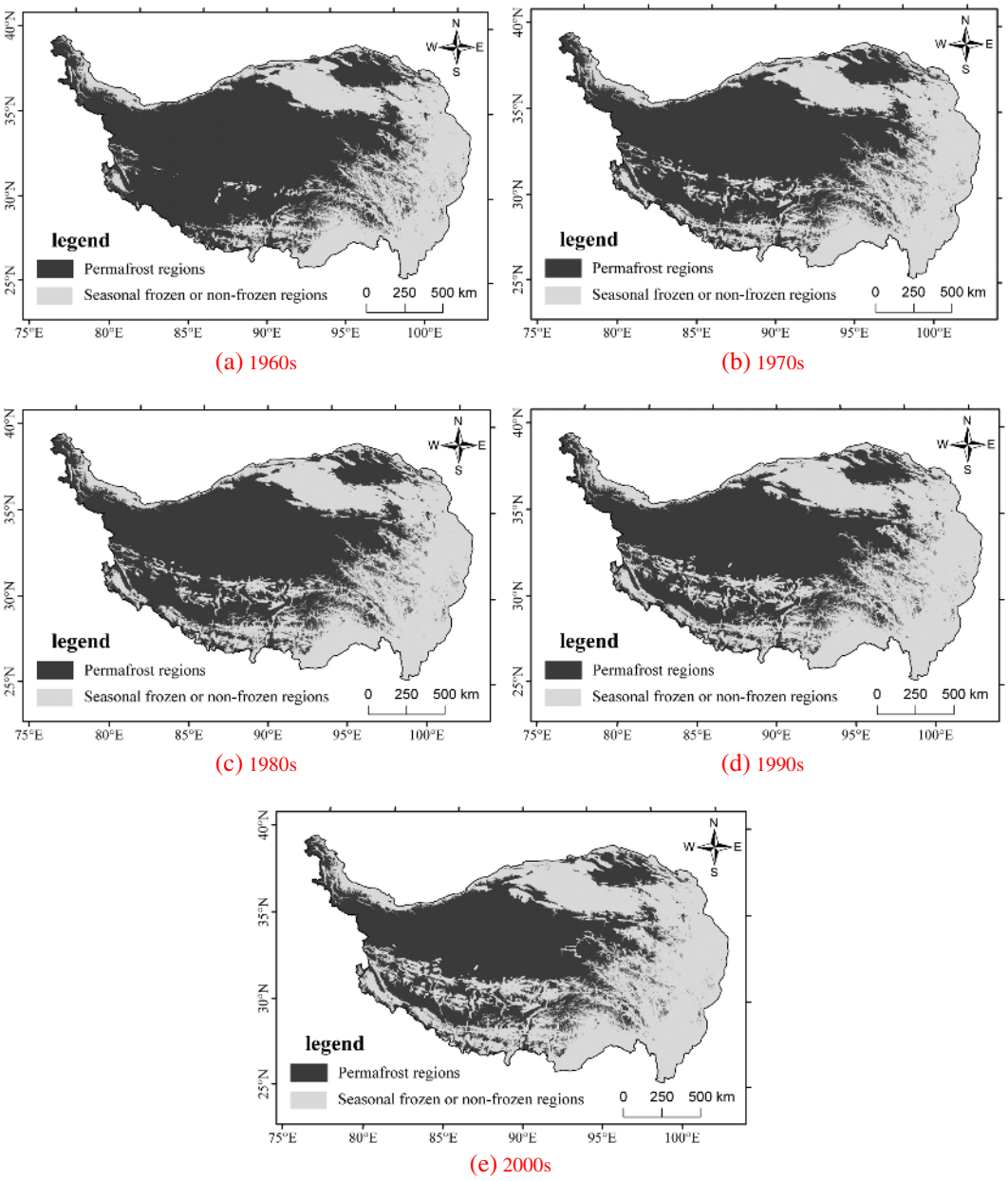

Figure 3 (a–e) Simulation results of permafrost distribution in each decade over the past 50 years on the Qinghai-Tibet Plateau.

Table 4 Total areas of permafrost on the QTP in each decade.

	1960s	1970s	1980s	1990s	2000s
Area ($\times 10^6$ km^2)	1.60	1.49	1.45	1.36	1.27

See text for abbreviation.

Considering these factors, the simulation results for the total areas of permafrost distribution on the QTP are generally consistent with existing permafrost maps.

Taking the *1:3 M Permafrost Map on the QTP* (Li & Cheng, 1996) as an example, the difference in permafrost distribution between the map and the simulation results in the 1990s was 15.2 per cent of the total permafrost area.

Comparison between the Simulation Model and other Simulation Methods

There are two main methods for simulating permafrost distribution on the QTP, one based on the altitudinal model and the other based on mean annual ground temperature (MAGT) data. Through experiments, Wu *et al*. (2000) and Zhao *et al*. (2007) confirmed that the simulation results based on altitudinal methods have a higher accuracy than

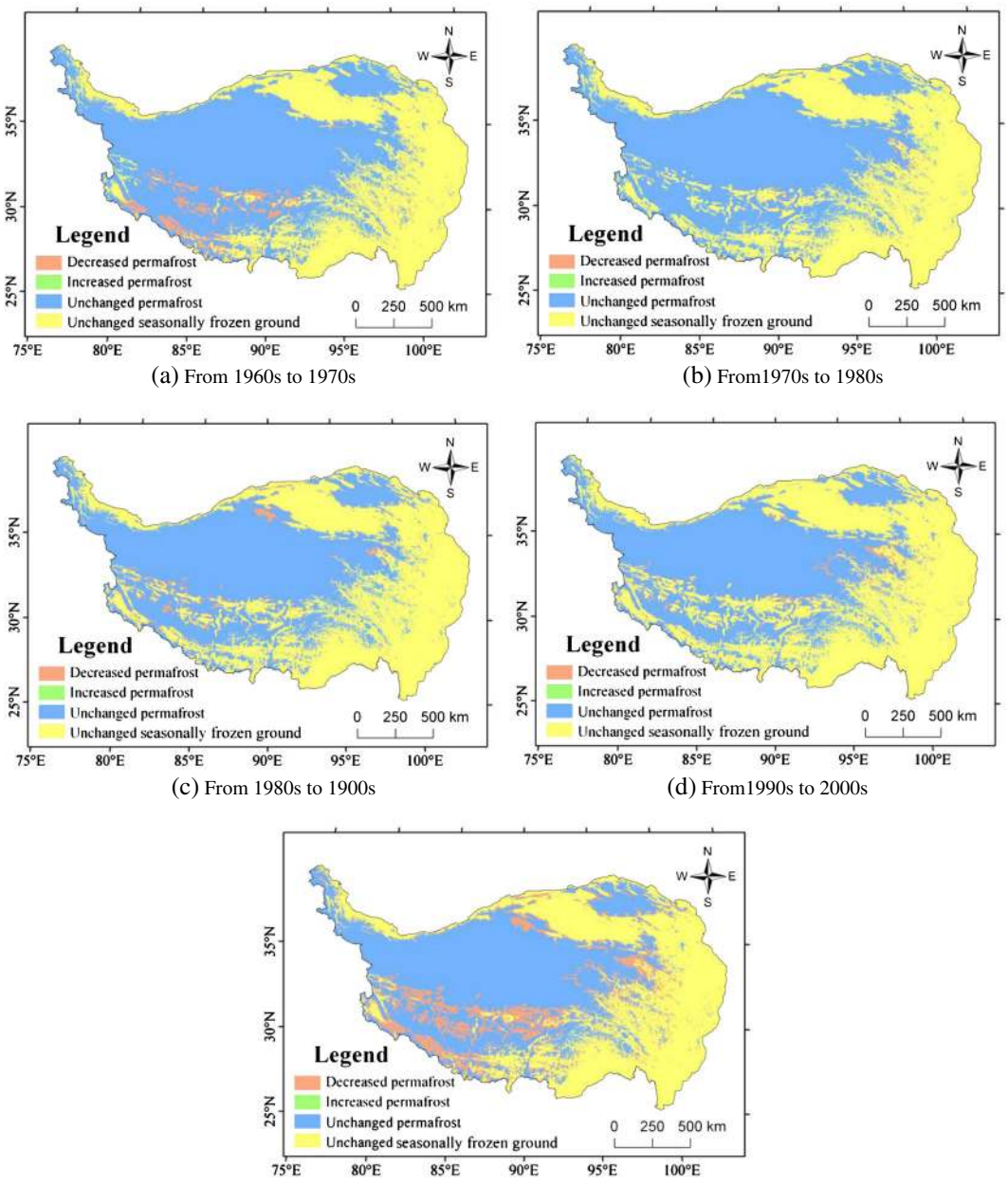

(a) From 1960s to 1970s

(b) From1970s to 1980s

(c) From 1980s to 1900s

(d) From1990s to 2000s

(e) From 1960s to 2000s

Figure 4 (a–e) Spatial distribution change in permafrost on the Qinghai-Tibet Plateau over the past 50 years. Decreased permafrost: permafrost that has degraded to seasonally frozen ground; Increased permafrost: seasonally frozen ground that has transformed to permafrost; Unchanged permafrost: permafrost that has persisted over a particular time period; Unchanged seasonally frozen ground: persistently non-permafrost conditions. This figure is available in colour online at wileyonlinelibrary.com/journal/ppp

Table 5 Decadal areas ($\times 10^3$ km^2) of frozen ground over the past 50 years.

Time period	Decreased permafrost	Increased permafrost	Unchanged permafrost	Unchanged seasonally frozen ground
1960s–1970s	117.4	1.8	1483.7	1051.2
1970s–1980s	34.8	3.1	1450.7	1165.5
1980s–1990s	92.7	0.6	1361.1	1199.7
1990s–2000s	95.1	0.0	1266.6	1292.4
1960s–2000s	334.7	0.2	1266.4	1052.8

Table 6 Total areas of permafrost on the QTP from published sources.

Source	Area ($\times 10^6$ km^2)	Period	Note
Zhou and Guo (1982)	1.50	1970s	*Permafrost Map of China* (compiled in 1975)
Xu and Wang (1983)	1.49	1970s	1:4 M *Permafrost Map of China* (compiled in 1978)
Shi (1988)	1.50	1970s	1:4 M *Snow, Ice and Permafrost Map of China* (1988)
Wang (1997)	1.23	1990s	1:3 M *Permafrost Map on the QTP* (Li and Cheng, 1996)
Cheng and Liu (2008)	1.28	2000s	Simulated using MAGT data
World Data Centre for Glaciology and Geocryology (2010)	1.33	2000s	Including foreign areas

See text for abbreviations.

those based on MAGT data. Nevertheless, the altitudinal model cannot simulate permafrost distribution on the QTP at different time periods. Based on the altitudinal model, the response model is presented, verified and widely used to simulate permafrost distribution on the QTP at different time periods (Li & Cheng, 1999; Jin *et al.*, 2000). Compared with the previous response model (Li & Cheng, 1999), our simulation method has the following merits:

(1) Our simulation method has a higher precision and quality. The model input data (MAAT, DEM and VLRT) are better constrained than in previous studies. For example, MAAT data in the present study are based on observations at meteorological stations rather than predictions made in previous studies. Additionally, the data in this study have a much higher spatial resolution (about 500 m) than those in previous studies (about 50 000 m).
(2) Our simulation results have more significance for understanding previous changes in permafrost distribution on the QTP. Most previous simulation studies predict permafrost distribution on the QTP at some time point in the future, such as in 2009, 2049 and 2009, so the time span is large. By contrast, in this research, permafrost distribution is simulated in a long time series over the past 50 years, which is more useful for understanding the changes that have already taken place on the QTP.

CONCLUSIONS

Based on the response model, the decadal permafrost distribution on the QTP was simulated over the past 50 years using SRTM3, MAAT and VLRT data. Through comparison with published permafrost maps and previous simulation studies, we think that the simulation results are reasonable and provide a basis for understanding changes in permafrost distribution in a long time series.

The areas of simulated permafrost on the QTP in the 1960s, 1970s, 1980s, 1990s and 2000s are 1.60×10^6 km^2, 1.49×10^6 km^2, 1.45×10^6 km^2, 1.36×10^6 km^2 and 1.27×10^6 km^2, respectively. The total area of permafrost has continuously declined during this overall time period, and the rate of permafrost loss has accelerated since the 1980s (Table 5). The simulated areas of persistent permafrost are mainly distributed in the Qilian Mountains and on the central and western QTP, while degraded permafrost regions are mainly distributed in the boundary regions between permafrost and seasonally frozen ground.

The simulation model in this research is a scenario type, so the simulated results are for steady-state permafrost conditions. In order to evaluate the response of altitudinal permafrost to climate change, we should now develop simulation models which can accommodate time lags and ground ice conditions.

ACKNOWLEDGEMENTS

This research was supported by the National Science Technology Support Plan Project (2012BAH28B01-03), the National Natural Science Foundation of China (41171332, 40830529) and the National Science Technology Basic Special Project (2011FY110400-2). We would like to express our gratitude to the editors and the anonymous reviewers for suggestions that improved our paper.

REFERENCES

Bartier PM, Keller CP. 1996. Multivariate interpolation to incorporate thematic surface data using inverse distance weighting (IDW). *Computers & Geosciences* **12**: 795–799. DOI: 10.1016/0098–3004(96)00021–0

Bonnaventure PP, Lewkowicz AG. 2010. Modelling climate change effects on the spatial distribution of mountain permafrost at three sites in northwest Canada. *Climatic Change* **105**: 293–312. DOI: 10.1007/s10584–010–9818–5

Bonnaventure PP, Lewkowicz AG, Kremer M, Sawada MC. 2012. A permafrost probability model for the southern Yukon and northern British Columbia, Canada. *Permafrost and Periglacial Processes* **23**: 52–68. DOI: 10.1002/ppp.1733

Cheng GD. 1984. Problems on zonation of high-altitudinal permafrost. *Acta Geographica Sinica* **39**: 185–193 (in Chinese).

Cheng ZG, Liu XD. 2008. A preliminary study of future permafrost distribution on the Qinghai-Tibet Plateau under global warming conditions. *Areal Research and Development* **27**: 80–85 (in Chinese). PII: 1003–2363 (2008) 06–0080–06

Cheng GD, Wu TH. 2007. Responses of permafrost to climate change and their environmental significance, Qinghai-Tibet Plateau. *Journal of Geophysical Research* **112**: F02S03. DOI: 10.1029/2006JF000631

Delisle G, Caspers G, Freund H. 2003. Permafrost in north-central Europe during the Weichselian: How deep? In *Permafrost*, Phillips M, Springman S, Arenson L (eds). Swets & Zeitlinger: Lisse; 187–191.

Ding DW, Xu XZ. 1982. On regionalization indexes of horizontal distribution of permafrost in China. In *Proceedings of the Symposium on Glaciology and Cryopedology held by Geographical Society of China (Cryopedology)*, Lanzhou Institute of Glaciology and Cryopedology, Chinese Academy of Sciences (eds). Science Press: Beijing; 70–73 (in Chinese).

Jiang ZX. 1982. Discussion on the mathematical models of physic-geographical zonation. *Acta Geographica Sinica* **37**: 98–103 (in Chinese).

Jiang FC, Wu XH, Wang SB, Zhao ZZ, Fu JL. 2003. Basic features of spatial distribution of the limits of permafrost in China. *Journal of Geomechanics* **9**: 303–312 (in Chinese). PII: 1006–6616(2003)04–0303–10

Jin HJ, Li SX, Cheng GD, Wang SL, Li X. 2000. Permafrost and climatic change in China. *Global and Planetary Chang* **26**: 387–404. PII: S0921–8181_00.00051–5

Lewkowicz AG, Ednie M. 2004. Probability mapping of mountain permafrost using the BTS method, Wolf Creek, Yukon Territory, Canada. *Permafrost and Periglacial Process* **15**: 67–80. DOI: 10.1002/ppp.480

Li BY. 1987. On the extent of the Qinghai-Xizang (Tibet) Plateau. Geographical Research **6**: 57–64 (in Chinese).

Li SD, Cheng GD. 1996. *1:3 M Permafrost Map on the QTP*. Gansu Culture Press: Lanzhou.

Li X, Cheng GD. 1999. A GIS-aided response model of high-altitude permafrost to global change. *Science in China (D)* **42**: 72–79.

Li QY, Xie ZC. 2006. Analyses on the Characteristics of the Vertical Lapse Rates of Temperature. *Journal of Shihezi University (Natural Science)* **24**: 719–723 (in Chinese). PII: 1007–7383 (2006) 06–0719–05

Li JJ, Zheng BX, Yang XJ, Xie YQ, Zhang LY, Ma ZH, Xu SY. 1986. *Glaciers of Xizang (Tibet)*. Science Press: Beijing (in Chinese).

Li X, Cheng GD, Chen XZ. 1998. Response of permafrost to global change on the Qinghai-Xizang Plateau — A GIS-aided model. In *Permafrost – Seventh International Conference (Proceedings)*, Lewkowicz AG, Allard M (eds). Centre d'études nordiques, Université Lavall: Québec; 657–661.

Li X, Cheng GD, Wu QB, Ding YJ. 2003. Modeling Chinese cryospheric change by using GIS technology. *Cold Regions Science and Technology* **36**: 1–9. DOI: 10.1016/S0165–232X(02)00075–7

Li X, Cheng GD, Jin HJ, Kang E, Che T, Wu LZ, Nan ZT, Wang J, Shen YP. 2008. Cryospheric change in China. *Global and Planetary Change* **62**: 210–218. DOI: 10.1016/j.gloplacha.2008.02.001

Lu GY, Wong DW. 2008. An adaptive inverse-distance weighting spatial interpolation technique. *Computers & Geosciences* **34**: 1044–1055.

Malevsky-Malevich SP, Molkentin EK, Nadyozhina ED, Shklyarevich OB. 2001. Numerical simulation of permafrost parameters distribution in Russia. *Cold Regions Science and Technology* **32**: 1–11. PII: S0165–232X(01)00018–0

Markus I. 1996. Modeling and Verification of the Permafrost Distribution in the Bernese Alps (Western Switzerland). *Permafrost and Periglacial Processes* **7**: 267–280. PII: 1045–6740/96/030267–14

Nan ZT, Gai ZS, Li SX, Wu TH. 2003. Permafrost Changes in the Northern Limit of Permafrost on the Qinghai-Tibet Plateau in the Last 30 Years. *Acta Geographica Sinica* **58**: 817–823 (in Chinese).

Nan ZT, Li SX, Cheng GD. 2005. Prediction of permafrost distribution on the Qinghai-Tibet Plateau in the next 50 and 100 years. *Sciences in China (D)* **48**: 797–804. DOI: 10.1360/03 yd0258

Niu WY. 1980. Theoretical analysis on physic-geographical zonation. *Acta Geographica Sinica* **35**: 288–298 (in Chinese).

Salzmann N, Frei C, Vidale PL, Hoelzle M. 2007. The application of Regional Climate Model output for the simulation of high-mountain permafrost scenarios. *Global and Planetary Change* **56**: 188–202. DOI: 10.1016/j.gloplacha.2006.07.006

Shi YF. 1988. *Map of Snow, Ice and Frozen Ground in China*. China Cartographic Publishing House: Beijing.

Wang SL. 1997. Study on permafrost degradation in the Qinghai-Xizang Plateau. *Advances in Earth Sciences* **12**: 164–167 (in Chinese).

Wang SL, Jin HJ, Li SX, Zhao L. 2000. Permafrost degradation on the Qinghai-Tibet Plateau and its environmental impacts. *Permafrost and Periglacial Process* **11**: 43–53.

World Data Centre for Glaciology and Geocryology. 2010. The Type of Permafrost and Frozen Ground. WDC for Glaciology and Geocryology, Lanzhou. http://wdcdgg.westgis.ac.cn/DATABASE/ccreis/QZPLAT/frozen%20ground.htm [20 June 2010]

Wu QB, Li X, Li WJ. 2000. Computer simulation and mapping of the regional distribution of permafrost along the Qinghai-Xizang Highway. *Journal of Glaciology and Geocryology* **22**: 323–326 (in Chinese). PII: 1000–0240 (2000) 04–0323–04

Wu QB, Li X, Li WJ. 2001. The Response Model of Permafrost along the Qinghai–Tibetan Highway under Climate Change. *Journal of Glaciology and Geocryology* **23**: 1–6 (in Chinese). PII: 1000–0240 (2001) 01–0001–06

Wu JC, Sheng Y, Wu QB, Wen Z. 2009. Process and modes of permafrost degradation on the Qinghai-Tibet Plateau. *Science in China (D)* **39**: 1570–1578 (in Chinese). DOI: 10.1007/s11430–009–0198–5

Xu XZ, Wang JC. 1983. Preliminary discussion on the distribution of frozen ground and its zonality in China. In *Proceedings of 2nd National Conference on Permafrost (Selection)*, Lanzhou Institute of Glaciology and Cryopedology, Chinese Academy of Sciences (eds). Gansu People's Publishing House: Lanzhou; 3–12.

Yang YC, Li BY, Yin ZS. 1983. *Geomorphology of Xizang (Tibet)*. Science Press: Beijing.

Yang M, Nelson, FE, Shiklomanov NI, Guo D, Wan G. 2010. Permafrost degradation and its environmental effects on the Tibetan Plateau: A review of recent research. *Earth-Science Reviews* **103**: 31–44. DOI: 10.1016/j.earscirev.2010.07.002

Zhang YL, Li BY, Zheng D. 2002. A discussion on the boundary and area of the Tibetan Plateau in China. *Geographical Research* **21**: 1–8 (in Chinese). PII: 1000–0585 (2002) 01–0001–10

Zhao SM, Cheng WM, Chai HX, Qiao YL. 2007. Research on the information extraction method of periglacial geomorphology on the Qinghai-Tibet Plateau based on remote sensing and SRTM: A case study of 1:1,000,000 Lhasa map sheet (H46). *Geographical Research* **26**: 1175–1185 (in Chinese). PII: 100020585 (2007) 0621175212

Zhao L, Ding YJ, Liu GY, Wang SL, Jin HJ. 2010. Estimates of the Reserves of Ground Ice in Permafrost Regions on the Tibetan Plateau. *Journal of Glaciology and Geocryology* **32**: 1–9 (in Chinese). PII: 1000–0240 (2010) 01–0001–09

Zhou YW, Guo DX. 1982. Major features of permafrost in China. *Journal of Glaciology and Geocryology* **4**: 1–19 (in Chinese).

